

Summary

The drag produced by trapped lee waves in flow over an axisymmetric mountain is explicitly calculated for 2-layer atmospheres where the stratification is either stronger in the lower layer and weaker in the upper layer, or neutral in the lower layer and stable in the upper layer, with a sharp temperature inversion in between. In both cases, the drag is produced simultaneously by waves that propagate in the upper layer, and 3D lee waves (trapped in the lower layer in the first case and trapped at the inversion in the second), which form a “ship-wake” pattern originating above the obstacle downstream of the mountain. Because of additional directional wave dispersion effects relative to the corresponding 2D flow, the drag enhancement in resonant conditions is less pronounced. However, the drag may still take values well above the hydrostatic limit valid if the upper stably stratified layer extended down to the surface, with a sizeable contribution coming from trapped lee waves. The results obtained using linear theory are compared with numerical simulations, showing good agreement.

1. Introduction

In global numerical weather and climate prediction models, the drag associated with trapped lee waves is typically not represented, either explicitly (because the associated waves are not resolved) or in the orographic drag parametrization scheme (because these waves are hard to parametrize). However, there are reasons to believe that this drag is important, and that it may be mistakenly represented in these models by artificially increasing the boundary layer drag, which accounts for different physical processes and has a distinct dependence on the flow parameters. Smith [1] derived a generic expression for the drag associated with trapped lee waves in flow over a 2D ridge, and Gregory et al. [2] extended this expression to flow over 3D orography. However, these expressions did not allow a systematic exploration of parameter space. Teixeira et al. [3] and Teixeira et al. [4] explored the drag behaviour as a function of flow parameters for flow over a 2D ridge, for a 2-layer atmosphere akin to that adopted by Scorer [5], i.e. with higher static stability in the lower layer and lower static stability in the upper layer (Case 1) and for the atmosphere of Vosper [6], i.e. with neutral stability in the lower layer, stable stratification in the upper layer, and an inversion in between (Case 2), respectively. Here, this approach is extended to flow over an axisymmetric mountain.

2. Theoretical Model

The flow is assumed to be inviscid, non-rotating, and linearized. Variations of the wind with height are ignored and the wave trapping mechanism is due to the variation of the static stability with height. The Taylor-Goldstein equation then takes the form:

$$\hat{w}'' + \frac{(k_1^2 + k_2^2)}{k_1^2} (l^2 - k_1^2) \hat{w} = 0 \quad (1)$$

where \hat{w} is the Fourier transform of the vertical velocity perturbation associated with the waves, $l=N/U$ is the Scorer parameter (where U and N are, respectively, the wind velocity and Brunt-Vaisala frequency of the incoming flow), and (k_1, k_2) is the horizontal wavenumber vector of the waves. The solution to this equation must satisfy a free-slip boundary condition at the surface:

$$\hat{w}(z=0) = iUk_1 \hat{h} \quad (2)$$

where \hat{h} is the Fourier transform of the surface elevation. A radiation or wave decay boundary condition as $z \rightarrow \infty$, and conditions prescribing the continuity of \hat{w} and of the pressure (or its Fourier transform) at the interface between the two atmospheric layers are prescribed. These layers are defined for Case 1 and Case 2 by the potential temperature profiles shown in Figure 1. l_1 and l_2 are the Scorer parameters in the lower and upper layer. H is the height of the lower layer. The ultimate aim is to calculate the value of the drag, given by:

$$D = 4\pi^2 i \int \int k_1 \hat{p}^* (z=0) \hat{h} dk_1 dk_2 \quad (3)$$

where \hat{p} is the Fourier transform of the pressure perturbation. For Case 1, the resonance condition for the existence of trapped lee waves is

$$\tan(m_1 H) = -\frac{m_1}{n_2} \quad (4)$$

whereas for Case 2, the resonance condition is instead

$$\tanh(k_{12} H) = \frac{k_{12} H}{Fr^{-2}(k_{12}^2/k_1^2) - n_2 H} \quad (5)$$

where m_1 and n_2 are, respectively, the vertical wavenumber of the waves trapped in the lower layer and the equivalent vertical wave decay rate in the upper layer, $k_{12} = (k_1^2 + k_2^2)^{1/2}$ and $Fr = U/(g'H)^{1/2}$ is a Froude number, where $g' = g\Delta\theta/\theta_0$ is the reduced gravity based on the temperature jump at the inversion. In either case, these conditions enable the double integral in (3) to become a single integral for the trapped lee wave drag contribution.

3. Results (Case 1 – Scorer’s atmosphere)

The drag normalized by the hydrostatic value it would have if the lower layer extended indefinitely is shown in Figure 2 as a function of $l_1 H$, for $l_2/l_1=0.2$ and different $l_1 a$. The drag oscillates with $l_1 H$, attaining maxima near $l_1 H/\pi = 0.5 + n$, where n is an integer, and minima in between, due to constructive and destructive interference of upward and downward propagating waves, respectively. Drag maxima produced by trapped lee waves tend to occur for slightly higher $l_1 H$ than those produced by vertically propagating waves, and become more dominant as $l_1 a$ decreases. The trapped lee wave drag takes values exceeding the hydrostatic one-layer limit.

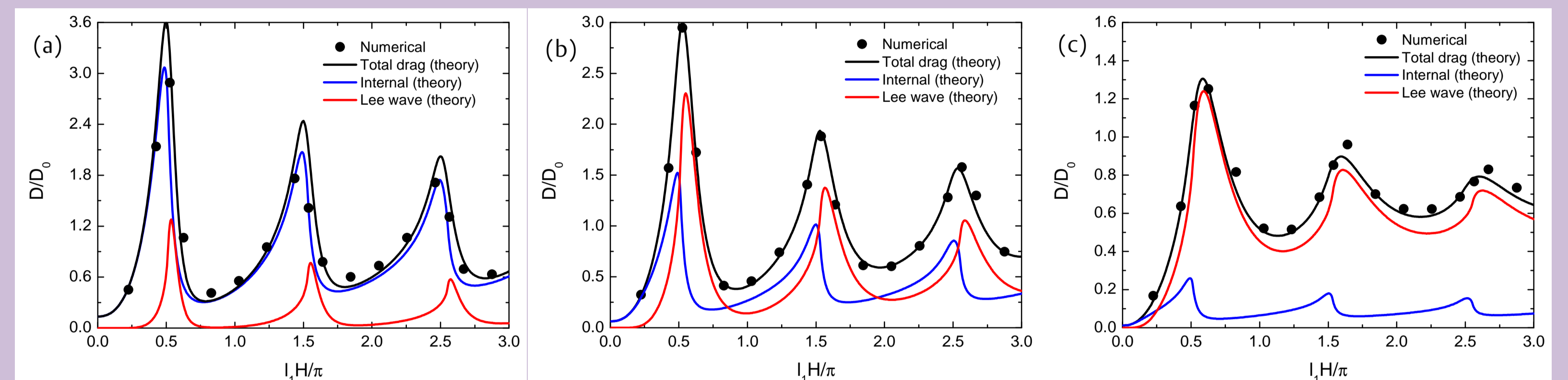


Figure 2. Normalized drag as a function of $l_1 H/\pi$ for $l_2/l_1=0.2$. (a) $l_1 a=10$, (b) $l_1 a=5$, (c) $l_1 a=2$.

Figure 3 shows horizontal cross-sections of w at $z=H/2$ for $l_2/l_1=0.2$ and $l_1 H/\pi=0.5$ (first drag maximum). The trapped lee waves (which in this case are internal waves propagating horizontally in the lower layer) form a triangular wake downstream of the mountain, reminiscent of a ship wake. Clearly, the wave structure is reproduced, at least qualitatively, by the analytical solution, which in principle should only be valid for $x/H \gg 1$.

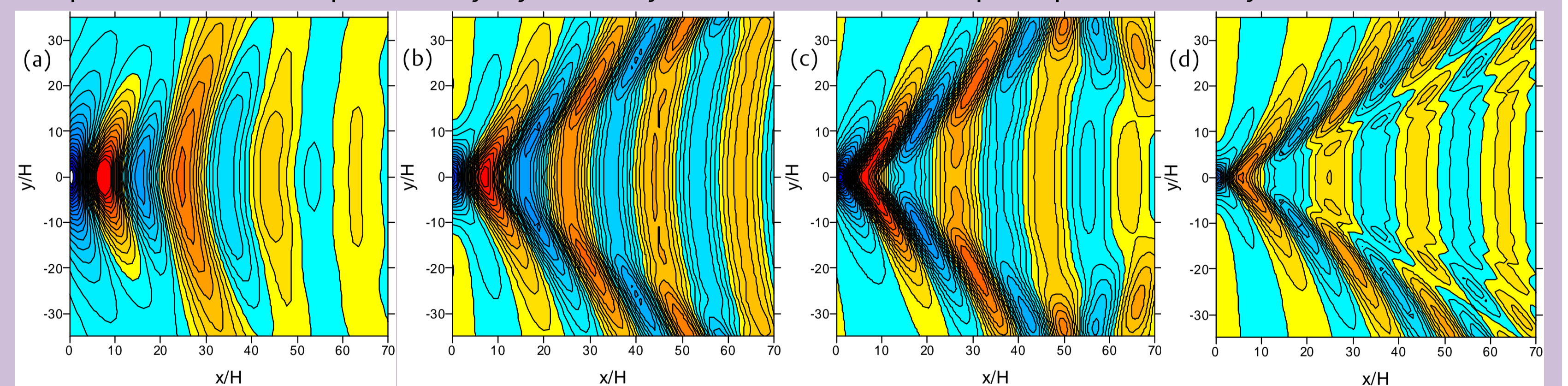


Figure 3. Horizontal cross-sections of w at $z=H/2$ for $l_1 H=0.5$ and $l_2/l_1=0.2$. (a),(c) Numerical, (b),(d) analytical. (a),(b) $l_1 a=5$, (c),(d) $l_1 a=2$.

3. Results (Case 2 – Vosper’s atmosphere)

Figure 4 shows the drag as a function of Fr normalized by its hydrostatic value valid if the upper layer extended down to the surface, for $l_2 H=0.5$ and different values of $l_2 a$. Unlike in Case 1, the normalized drag has one single maximum, occurring in the vicinity of $Fr=1$, but this maximum can also exceed 1. The trapped lee wave drag is concentrated predominantly for $Fr < 1$, while the drag associated with internal waves occurs mostly for $Fr > 1$. Again, the trapped lee wave drag becomes more dominant over the internal wave drag as $l_2 a$ increases (i.e. the flow becomes more non-hydrostatic). Figure 5 shows cross sections of w for $z=H$ (the inversion where the

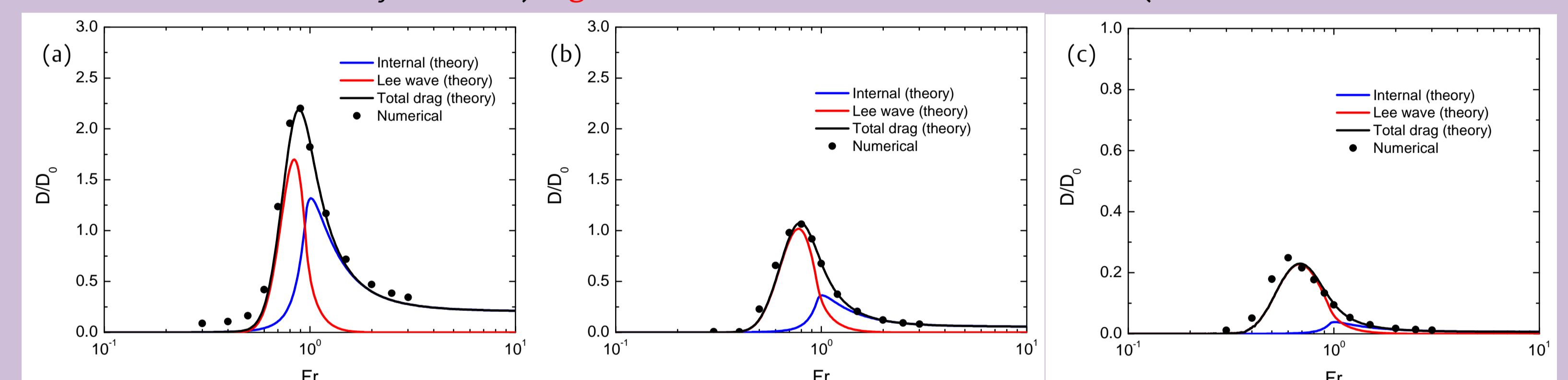


Figure 4. Normalized drag as a function of Fr for $l_2 H=0.5$. (a) $l_2 a=2$, (b) $l_2 a=1$, (c) $l_2 a=0.5$.

trapped lee waves propagate). Also here, there is a triangular wake originating over the mountain akin to a ship wake, which is well reproduced by the analytical model for both values of $l_2 a$ considered.

Case 1 and Case 2 show that the total drag results from a superposition between the trapped lee wave drag and the internal gravity wave drag, however, the former drag acts at lower levels in the atmosphere.

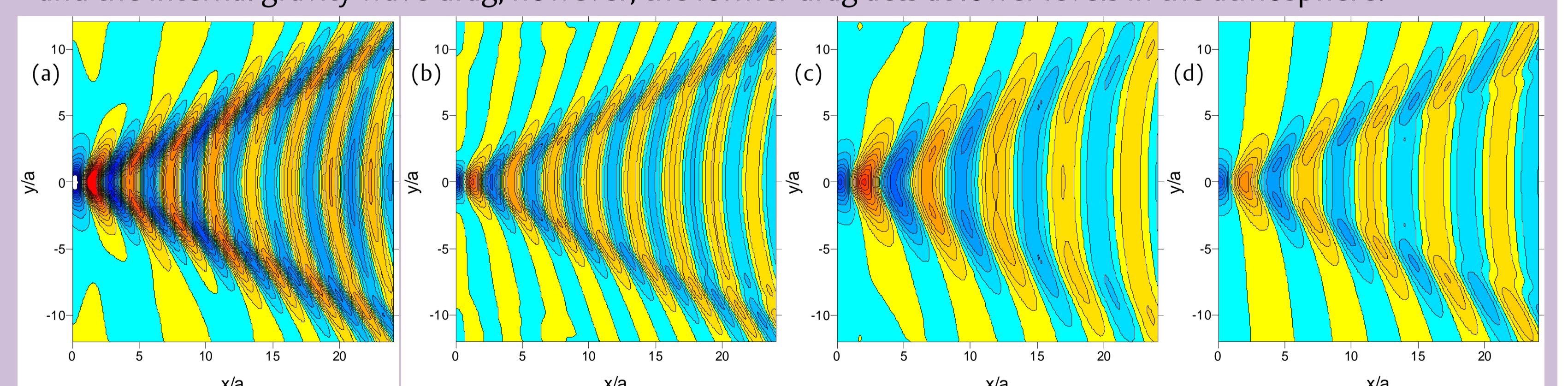


Figure 5. Horizontal cross-sections of the w at $z=H$ for $Fr=0.85$ and $l_2 H=0.5$. (a),(c) Numerical, (b),(d) analytical. (a),(b) $l_2 a=2$, (c),(d) $l_2 a=1$.

Conclusions

For the preceding results using idealized two-layer atmospheres, it is clear that trapped lee wave drag gives a substantial contribution to the total drag, larger than the hydrostatic single-layer limit, as long as the flow conditions are tuned to lead to resonant drag enhancement by constructive wave interference. It therefore seems necessary to consider the effect of trapped lee waves in drag parametrizations used in weather and climate prediction models, especially as their resolution increases to $O(10\text{km})$ or above. The trapped lee wave drag calculations presented here pave the way for the development of such representations, as it is straightforward to extend them to the mountains with an elliptical horizontal cross-section used in parametrization schemes through a simple coordinate transformation.

References

- [1] Smith, R.B. (1976) The generation of lee waves by the Blue Ridge. *J. Atmos. Sci.*, **33**, 507-519
- [2] Gregory, D., Shutts, G.J. and Mitchell, J.R. (1998) A new gravity wave drag scheme incorporating anisotropic orography and low-level wave breaking: impact upon the climate of the UK Meteorological Office Unified Model. *Q. J. R. Meteor. Soc.*, **124**, 463-493
- [3] Teixeira, M.A.C., Argain, J.L., Miranda, P.M.A. (2013) Drag produced by trapped lee waves and propagating mountain waves in a two-layer atmosphere. *Q. J. R. Meteor. Soc.*, **139**, 964-981
- [4] Teixeira, M.A.C., Argain, J.L. and Miranda, P.M.A. (2013) Orographic drag associated with lee waves trapped at an inversion. *J. Atmos. Sci.*, **70**, 2930-2947
- [5] Scorer, R.S. (1949) Theory of waves in the lee of mountains. *Q. J. R. Meteor. Soc.*, **75**, 41-56
- [6] Vosper, S. B. (2004) Inversion effects on mountain lee waves. *Q. J. R. Meteor. Soc.*, **130**, 1723-1748